LA-UR -91-1652

1-5

LA-UR--91-1652

DE91 013029

Los Alamos National Laboratory is operated by the University of California for the United States Department of Energy under contract W 7405 ENG 36

TITLE DYNAMIC STRENGTH AND STRAIN RATE EFFECTS ON FRACTURE BEHAVIOR OF TUNGSTEN AND TUNGSTEN ALLOYS

AUTHOR(S) Anna K. Zurek and George T. Gray

SUBMITTED TO Proceedings of "DYMAT 91" Conference
. rasbourg, October 14-18, 1991

DISCLAIMER

This report was prepared as an account of work sponsored by an agency of the United States Government. Neither the United States Government nor any agency thereof, nor any of their employees, makes any warranty, express or implied, or assumes any legal liability or responsibility for the accuracy, completeness, or usefulness of any information, apparatus, product, or process disclosed, or represents that its use would not infringe privately owned rights. Reference herein to any specific commercial product, process, or service by trade name, trademark, manufacturer, or otherwise does not necessarily constitute or imply its endorsement, recommendation, or favoring by the United States Government or any agency thereof. The views and opinions of authors expressed herein do not necessarily state or reflect those of the United States Government or any agency thereof.

Los Alamos National Laboratory
Los Alamos, New Mexico 87545

MASTER

DYNAMIC STRENGTH AND STRAIN RATE EFFECTS ON FRACTURE BEHAVIOR OF TUNGSTEN AND TUNGSTEN ALLOYS

Anna K. Zurek and George T. Gray III
Materials Science and Technology Division
Los Alamos National Laboratory
Los Alamos, New Mexico 87545

Abstract An investigation of the stress-strain response as a function of strain rate, spall strength, and dynamic fracture behavior of pure W, W-26Re, W-Ni-Fe and W-Ni-Fe-Co has been performed. Spall strength measurements, obtained in symmetric-impact tests, showed an increase in spall strength from 0.4 GPa for pure tungsten to 3.8 GPa for 90W-7Ni-3Fe. Concurrent with the increase in spall strength was a change in fracture mode from cleavage (for pure W) to a mixture of transgranular and intergranular fracture for the alloyed systems. Compression testing performed at strain rates from 10^{-3} s^{-1} to 3000 s^{-1} showed that pure tungsten exhibits a large strain rate sensitivity and almost no work hardening at tested strain rates. In contrast, W-26Re and W-Ni-Fe-Co displayed significant work hardening at all strain rates.

1. Introduction

Unlike pure tungsten, tungsten alloys possess a combination of strength and ductility, corrosion resistance, and machinability in addition to a high density which makes them very attractive for kinetic energy penetrators or for radiation shielding materials. Tungsten alloys such as W-Ni-Fe or W-Ni-Fe-Co consist of nearly spherical grains of bcc tungsten surrounded by a fcc matrix phase containing Ni, Fe, Co and W. Because of their unique properties there is increasing interest in these alloys. In recent years several investigators have studied the static and dynamic properties of tungsten alloys in as-sintered and swaged conditions [1-6]. Rabin and German [1] showed that increasing tungsten content in W composites results in strengthening and a drastic decrease in the ductility of the alloy. Bose, Sims and German [2] studied the influence of the test temperature and strain rate sensitivity (crosshead speed from 10^{-3} to 10^{3} mm/s) of a 90W-7Ni-3Fe alloy and showed that the strength increases slightly with strain rate while ductility decreases. However, as the test temperature increases the strain rate sensitivity of this alloy diminishes. Meyer and co-workers [3] evaluated the dynamic strength and ductility of tungsten alloys in the as-sintered and swaged conditions, showing for each alloy a characteristic increase in strength (sometimes twice the quasi-static value) and a decrease in ductility by increasing the strain rate from 10^{-3} to 5000 s^{-1}. Lankford et., al. [4] proposed a relationship between the strength and the fracture mode of explosively fractured tungsten composite alloys. This relationship indicated a change from cleavage fracture mode in the tungsten particles for low strength tungsten alloys to an interfacial tungsten tungsten, tungsten-matrix mode of fracture (combination of W cleavage and inter phase fracture) for high strength tungsten alloys.

In this study, we investigated the stress-strain response of W-26Re, W-Ni-Fe and W-Ni-Fe-Co alloys in contrast with pure W as a function of strain rate, spall strength and dynamic fracture behavior.

2. Experimental Procedure

The mechanical response of pure tungsten fabricated using powder metallurgy was studied in a cold worked and recrystallized condition. A W-26Re powder-metallurgy alloy (single-phase solid-solution alloy, grain size approximately 1-2 μm) and two W-Ni-Fe alloys, one containing Co additions, were produced by liquid-phase sintering of elemental powders. The W-Ni-Fe was in cold-rolled-plate form while the W-Ni-Fe-Co was in a heavily swaged condition. The chemical composition of the W-heavy alloys were: 90W-7Ni-3Fe and 93W-4.8Ni-2Fe-0.2Co. The final microstructures of the heavy alloys consisted of nominally 50 μm W particles surrounded by a soft Ni-Fe or Ni-Fe-Co matrix.

The quasi-static (strain rate 10^{-3} s^{-1}) and dynamic (strain rate of 2000 to 8000 s^{-1}) mechanical response were measured in compression using conventional a screw-driven testing frame and Split Hopkinson Pressure Bar, respectively. To evaluate the strain rate sensitivity of the W-based alloys the strength and the work hardening in compressive tests performed at strain rates of 10^{-3} s^{-1} and 2500-4000 s^{-1} were compared.

The dynamic spall strength was measured under dynamic uniaxial strain conditions, using an 80-mm gas gun at room temperature in vacuum (<1 Pa absolute pressure) [7]. In the spall test, the sample was subjected to a planar impact by a flyer plate, where both the sample and the flyer plate were fabricated from the test material. Upon impact of the flyer plate with the sample (target), a compressive shock wave propagates into the target as well as into the flyer. These waves reflect from the free back surfaces of both parts and propagate back into the sample. When two compressive waves meet (the incoming and reflected), a tensile wave is produced. If the pressure amplitude of this tensile wave exceeds the dynamic strength of the material it causes the sample to spall. In each test the impact pressure and the spall strength were measured using a manganin gauge (pressure gauge) as one branch of a Wheatstone bridge circuit in conjunction with a delayed triggering system to ensure a high signal-to-noise ratio. Projectile velocities (flyer plate velocities, measured using pressure transducers) in these tests were approximately 590 or 360 m/s, which yielded peak stresses of 25 and 15 GPa, respectively. The relative target-to-impactor thickness yielded a 1 μs stress pulse duration time and a spall fracture surface at the mid-section of the sample. The spalled fragments were recovered intact from a catch tank that was specially designed to simultaneously decelerate and cool the sample. This catch tank consisted of compartments of wool felt impregnated with water. Fractographic examination of all the spall fracture surfaces was performed using scanning electron microscopy (SEM).

3. Results and Discussion

Figures 1 thru 4 show the stress-strain response as a function of strain rate for the tungsten alloys studied. Table 1 summarizes the flow stress at 2% true strain for low and high strain rates, measured rate sensitivities at 2% true strain and calculated strain hardening rates for the highest strain rate available for the metals studied.

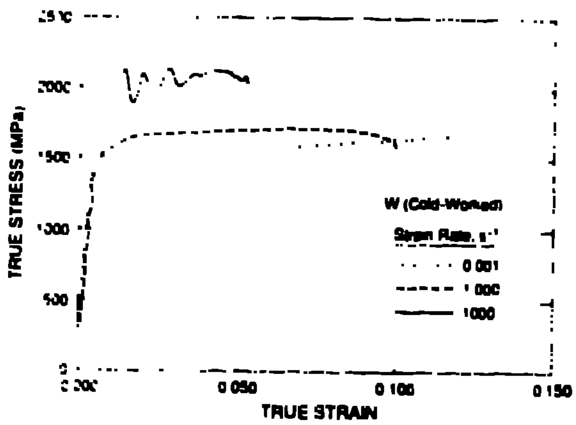

Fig. 1. Stress-strain response of cold-worked tungsten as a function of strain rate. Note the lack of strain hardening at all strain rates.

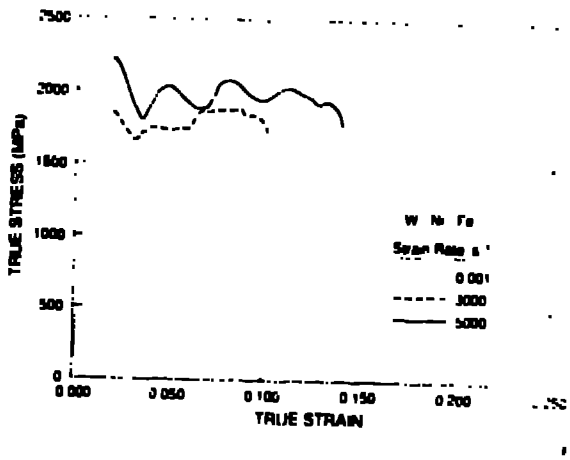

Fig. 2. Stress-strain response of W-Ni-Fe as a function of strain rate

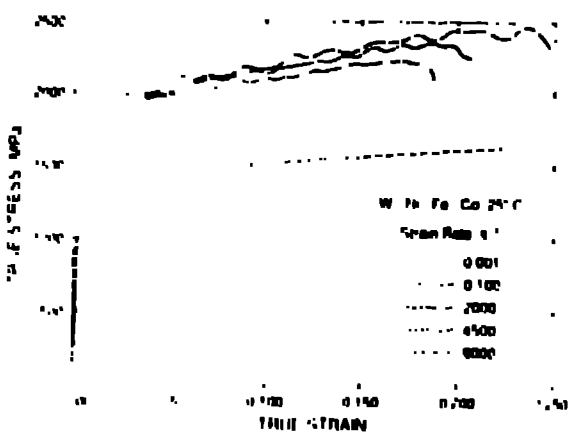

Fig. 3. Stress strain response of W Ni Fe Co as a function of strain rate.

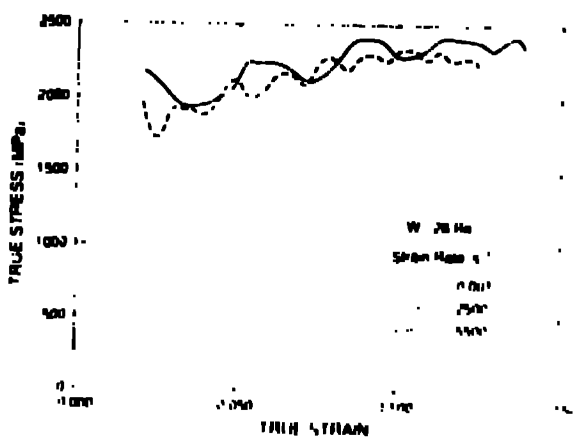

Fig. 4. Stress strain response of W 26Re (powder metallurgy material) as a function of strain rate.

The oscillations in data taken at high strain rate arise from elastic wave dispersion in the pressure bar.

TABLE 1

Metal	σ @ 2%ϵ (MPa) Low Rate	High Rate	$m = \frac{\delta \ln \sigma}{\delta \ln \dot{\epsilon}}$	Strain Hardening Rate @ High Rate (MPa per unit strain)
W(c-w)	1500	2000	.021	0
W(rec.)	900	1260	.023	0
W-Ni-Fe	1340	2000	.026	0
W-Ni-Fe-Co	1250	1950	.028	2720
W-26Re	1500	2000	.018	3075

The stress-strain response of all the tungsten-based alloys studied are observed to exhibit similar rate sensitivities of approximately 0.02. This magnitude of rate sensitivity is typical of many bcc and hcp metals which possess a high lattice resistance (Peierls barrier) to dislocation motion. The strain hardening rate measured at high strain rates in the tungsten and tungsten-based alloys varies. All materials studied showed stage I (region of easy dislocation glide) hardening. This observation is consistent with the 1963 study of Krock and Shepard [8] on the tensile behavior of liquid phase sintered W alloys. They concluded that the high rate of initial work hardening by the tungsten composite was closely associated with the properties of bcc tungsten. The pure tungsten, independent of starting condition, and the 90W-7-Ni-3Fe heavy-alloy displayed almost no stage II (region of linear hardening) strain hardening at high strain rate. The high-rate response of the W-Ni-Fe-Co and W-26Re alloys however, showed substantial hardening after yield. The differences in stage II work-hardening behavior in the W-alloys are consistent with previous studies of the work hardening of refractory metals [9]. Under quasi-static conditions, the lack of hardening in W and W-Ni-Fe may reflect material behavior near their saturation stress. A rough estimate of the saturation stress in a material can be made by taking approximately $3*10^{-3}$ [10] of the shear modulus multiplied by 3.09 (Taylor factor for a polycrystal). Using the shear modulus of 160 GPa for tungsten, gives an estimated saturation stress of approximately 1480 MPa. For pure tungsten this saturation stress is similar in magnitude to the maximum stress level achieved at quasi-static rates. The lack of stage II work-hardening in pure tungsten at high strain rate may be influenced by defect storage and defect interaction behavior. Suppressed motion of thermally-activated screw-dislocations at high-strain rate is similar to suppressed screw-dislocation motion at cryogenic temperatures [9]. The work-hardening in bcc metals at cryogenic temperatures may be low because of low screw-dislocation mobility and low secondary-dislocation activation [9]. While the edge dislocations are still mobile at high strain rates, they are incapable of producing significant hardening due to lack of dislocation interactions. Without significant motion of screw dislocations and secondary system activation, hardening should be low, consistent with our observations and low-temperature observations by others [9]. Addition of rhenium to tungsten is thought to alter the dislocation storage behavior and thereby increase work-hardening by increasing the edge-dislocation/interstitial interaction. While having only a minor influence on the yield stress, this will effectively raise the saturation stress.

The substantial strain hardening response of the W-Ni-Fe-Co compared to the W-Ni-Fe is postulated to be the result of two factors: Co additions and differences in the matrix microstructure. Co additions will supplement the substitutional hardening in the matrix, while the heavily swaged matrix should exhibit higher rate sensitivity compared to a lesser-worked matrix in W-Ni-Fe material. The increased hardening due to the Co may also reflect an increased saturation stress in the matrix. Both conditions are consistent with the slightly higher rate sensitivity and strong strain hardening response of the Co alloy system.

Table 2 lists the impact conditions and spall data for the materials studied.

TABLE 2

Material	Impact Velocity (m/s)	Shock Pressure (GPa)	Spall Strength (GPa)	Fracture Character
W(recrystallized)	590	25	0.4	Intergranular
W(cold rolled)	590	25	0.8	Cleavage
W-26Re (powder)	576	24	1.3	Intergranular
W-Ni-Fe	364	15	3.8	Ductile/
	366	15	3.4	transgranular

In Figures 5 and 6 examples are given of the stress-time spall trace and fractography accompanying spallation for the W-Ni-Fe and W-26Re alloys, respectively.

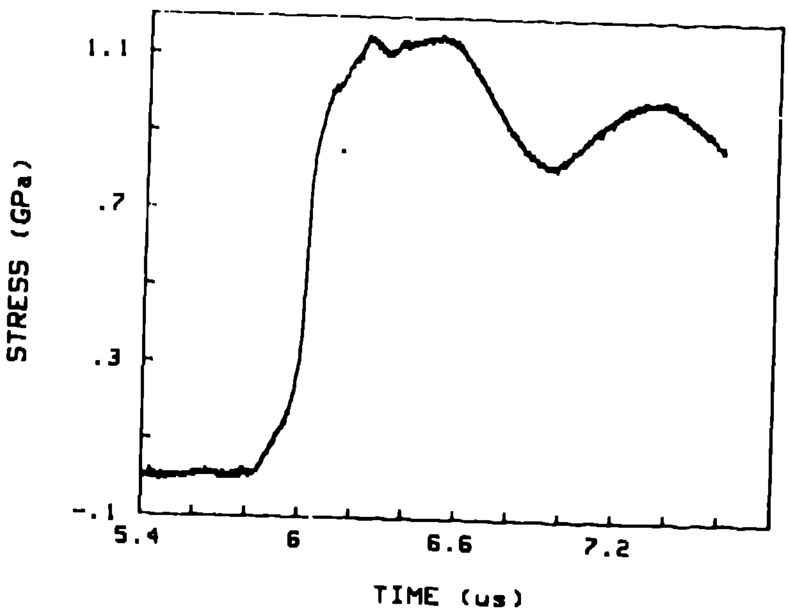

Fig. 5a. Stress-Time trace from spall test of W-Ni-Fe.

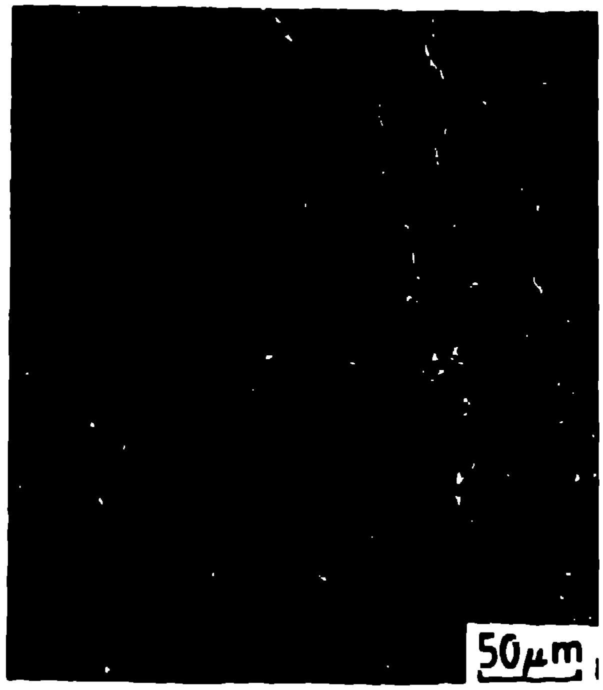

Fig. 5b. SEM micrograph of the fracture morphology in spalled W-Ni-Fe. Ductile

Fig. 6. SEM micrograph of the fracture morphology in spalled W-26Re. Intergranular fracture along prior powder grain boundaries.

The spall strength measurements in this study are consistent with the dynamic stress-strain response and general quasi-static fracture behavior of the W alloys studied. In the case of the recrystallized W, the notoriously poor ductility of this material under low or high-rate loading reflects the high strength, low work hardening, and sensitivity to impurities on the grain boundaries of this metal. The intrinsic high resistance to plastic flow in tungsten at ambient temperatures results in attainment of flow stress levels above the grain boundary fracture stress. This leads to intergranular fracture before significant plastic flow has occurred. Addition of mobile dislocations through cold-working and reduction in interstitial segregation to the grain boundaries improves this situation. This is reflected by the somewhat increased spall strength and change to cleavage fracture in the cold-worked tungsten. As Bechtolt and Shewmon [11] showed, there is a delicate balance between stress required for transgranular plastic flow compared with brittle intergranular separation. The W-26Re alloy exhibits an increased spall strength consistent with the increased rate of work-hardening of this alloy and the fine grain size which tends to suppress cleavage failure. The high spall strength of the W-Ni-Fe alloy is believed principally to reflect the strong influence of the ductile Ni-Fe matrix and W-matrix interface rather than the fracture behavior of the tungsten particles. As suggested by Krock and Shepard [8], the ductility of the W-Ni-Fe composite may be attributed in part to the crack arresting effect of the matrix layer which surrounds each W grain. The ductile-transgranular fracture morphology, as seen in the SEM fractograph Fig. 5b, shows that the spall fracture is concentrated in the matrix with only occasional fracture through tungsten particles.

4. Conclusions

Both pure W (recrystallized and cold worked) and W-Ni-Fe alloy in a cold rolled condition exhibit moderate quasi-static strength but a very low strain hardening capacity. In addition, pure W showed nearly zero spall strength and an intergranular and/or cleavage mode of fracture. W-26Re alloy demonstrated moderate spall strength. W Ni-Fe alloy showed high spall strength, almost comparable to the spall strength of pure copper [12]. An intergranular mode of fracture (W [illegible]Re) and ductile transgranular mode of fracture (W-Ni-Fe) were predominant in the alloys under dynamic uniaxial strain loading. W-26Re and W-Ni Fe alloys have very high quasi static strength and a high strain hardening rate characteristic.

Acknowledgments:

This research was performed under the auspices of the United States Department of Energy. Experimental contributions from C. E. Frantz, M. F. Lopez, C. Trujillo and W. Wright were most valuable. We wish to thank J. D. Embury for his interest and discussions on the subject of this manuscript.

References

1. Rabin, H. B., and German, R. M., Met. Trans. 19 A, 1988, pp. 1523-1532.

2. Bose, A., Sims, D., and German, R. M., Met. Trans. 19 A, 1988, pp. 487-494.

3. Meyer, L. W., Kunze, H.-D., and Staskewitsch, E., **Proc. of the Seventh International Ballistic Symposium,** The Hague-Netherlands, 1983, pp. 289-293.

4. Lankford, J., Anderson, C. E. Jr., Bodner S. R., J. of Materials Science Letters 7, 1988, pp. 1355-1358.

5. Meyer, L. W., Seifert K., and Kunze, H.-D., **Proc. of Fifth International Ballistic Symposium,** Toulouse-France April, 1980, pp. 200-204.

6. Tham, R., and Spilp, A. J., **Proc. of International Conference on Mechanical and Physical Behavior of Materials under Dynamic Loading, DYMET,** Ajaccio, Sep. 1988, pp. 85-90.

7. Zurek, A. K., Follansbee P. S., and Hack, J., Metall. Trans., **21**, 1990, pp.431-439.

8. Krock, R. H., and Shepard, L. A., Trans. Metal. Soc. AIME, **227**, 1963, pp. 1127-1134.

9. Arsenault, R. J., and Lawley, A.,: in Work Hardening, eds. Hirth, J. P., and Weertman, J., Gordon and Breach, NY (1968), p. 283.

10. A. D. Rollett, private communication.

11. Bechtold, J. H., and Shewmon, P. J., Trans. ASM, **46**, 1954, p. 397.

12. Zurek, A. K., Johnson, J. N., and Frantz, C. E., **Proceedings of the 2nd International Conference on Mechanical and Physical Behavior of Materials Under Dynamic Loading, Ajaccio France, Sept. 1988,** pp. 269-276.